

Contents lists available at [SciVerse ScienceDirect](http://www.sciencedirect.com)

# Environmental Pollution

journal homepage: [www.elsevier.com/locate/envpol](http://www.elsevier.com/locate/envpol)

## Arsenic fractionation in mine spoils 10 years after aided phytostabilization

Jurate Kumpiene<sup>a,\*</sup>, Jeffrey P. Fitts<sup>b</sup>, Michel Mench<sup>c</sup>

<sup>a</sup>Division of Waste Science and Technology, Luleå University of Technology, Luleå SE-97187, Sweden

<sup>b</sup>Environmental Sciences Department, Brookhaven National Laboratory, Upton, NY 11973-5000, USA

<sup>c</sup>UMR BIOGECO INRA 1202, Ecology of Communities, Bordeaux 1 University, Bât B2 RdC Est, Avenue des Facultés, F-33405 Talence, France

### ARTICLE INFO

#### Article history:

Received 9 November 2011

Received in revised form

13 February 2012

Accepted 17 February 2012

#### Keywords:

Iron

Selective dissolution

XANES

$\mu$ XRF mapping

### ABSTRACT

Aided phytostabilization using a combination of compost, zerovalent iron grit and coal fly ash (CZA) amendments and revegetation effectively promoted the biological recovery of mining spoils generated at a gold mine in Portugal. Selective dissolution of spoil samples in combination with solid phase characterization using microbeam X-ray absorption near edge structure ( $\mu$ XANES) spectroscopy and microbeam X-ray fluorescence ( $\mu$ XRF) mapping were used to assess As associations in spoils ten years after CZA treatment. The results show that As preferentially associates with poorly crystalline Fe-oxyhydroxides as opposed to crystalline Fe-(oxyhydr)oxide phases. The crystalline Fe(III)-phases dominated in the treated spoil and exceeded those of the untreated spoil three-fold, but only 2.6–6.8% of total As was associated with this fraction. Correlation maps of As:Fe reveal that As in the CZA-treated spoils is primarily contained in surface coatings as precipitates and sorbates. Arsenic binding with poorly crystalline Fe-oxyhydroxides did not inhibit As uptake by plants.

© 2012 Elsevier Ltd. All rights reserved.

### 1. Introduction

Mining operations have produced negative environmental consequences including soil contamination and ecosystem degradation (e.g. Hector and Rainer, 2010). The development of technologies to process lower-grade ores continues to increase the generation of mining waste. Mining waste accumulated in European Union countries alone has been estimated to total  $6 \cdot 10^9$  Mt (Lottermoser, 2003). Airborne particles from smelting sites have caused soil acidification and vegetation death over areas as large as several thousand hectares (Winterhalder, 1996). Non-vegetated land is prone to erosion and leaching processes that mobilize potentially toxic metal(loid)s and degrade surrounding ecosystems and groundwater resources.

The large scale of sites contaminated with mining wastes typically makes excavation and ex situ physical containment impractical. The in situ aided phytostabilization of large areas contaminated by mineral extraction and processing wastes offers an alternative strategy to contain and reduce risks to the environment and human health (Vangronsveld et al., 1995). Physical texture, chemical composition, macronutrient content, salinity, and

pH of mine spoils (the overburden, non-ore material from a mine) differ significantly from natural soils making spontaneous plant colonization extremely difficult and slow. Amendments that improve physico-chemical properties of spoils are therefore needed to establish stable vegetation.

Lime has traditionally been used to neutralize spoil acidity (Winterhalder, 1996), however, alternatives including low cost aluminosilicates, industrial alkaline residues and iron containing materials were demonstrated to more effectively reduce metal mobility, toxicity, and availability to plants leading to the establishment of a vegetative cover in mining-affected areas (Bleeker et al., 2002; Vangronsveld et al., 2000). In addition to site vegetation, amendments that improved microbial and enzyme activities were shown to further enhance development of a soil humus layer, which is absent in degraded mining sites, but necessary for soil functionality (Renella et al., 2008).

Zerovalent iron grit ( $\text{Fe}^0$ ) amendments, which rapidly oxidize to form Fe-oxyhydroxide phases in acidic spoils, have been previously shown to effectively reduce dissolved arsenic (As) by more than 90% (Hartley et al., 2004; Kumpiene et al., 2006). Potentiometric titrations and spectroscopic studies indicate that As adsorption occurs via ligand exchange with Fe-(hydr)oxide surface sites, predominantly forming bidentate inner-sphere complexes (Jain et al., 1999; Sherman and Randall, 2003). Poorly crystalline Fe-oxyhydroxide, such as ferrihydrite, having the largest specific surface area ( $600 \text{ m}^2 \text{ g}^{-1}$ ) (Dzombak and Morel, 1990) are the most

\* Corresponding author.

E-mail addresses: [jurate.kumpiene@ltu.se](mailto:jurate.kumpiene@ltu.se) (J. Kumpiene), [fitts@bnl.gov](mailto:fitts@bnl.gov) (J.P. Fitts), [mench@bordeaux.inra.fr](mailto:mench@bordeaux.inra.fr) (M. Mench).

reactive Fe-(hydr)oxide phases. Aging of metastable ferrihydrite results in the transformation to more crystalline phases (goethite, lepidocrocite, hematite), which have significantly lower specific surface area. Model system studies of the aging process have reported As desorption and increased leaching with age and increased crystallinity (Fuller et al., 1993; Pedersen et al., 2006), suggesting that the relative abundance of Fe-(hydr)oxide phases with different degrees of hydroxylation and crystallinity is an important factor controlling As stability in amended spoils. Other factors, such as pH, redox, organic acids, competing ions and presence of cationic metals are principally either facilitating or hindering As sorption to Fe oxides (Carabante et al., 2009; Meng et al., 2000; Redman et al., 2002).

Long-term experiments of aided phytostabilization are rare and primarily focus on the recovery of soil biological parameters (Vangronsveld et al., 2009). Studies of long-term solid-phase transformations in amended soils are even less common (e.g. Nachtegaal et al., 2005). Selective dissolution and extraction methods are commonly used to quantify the relative abundance of Fe-(hydr)oxide phases in soils according to their crystallinity (Dold, 2003). These fractions are subject to different dissolution scenarios leading to the release of associated elements. As with all chemical extraction methods, mineral phases and associated element fractions are operationally defined. Elements can be redistributed during extraction and/or falsely attributed to other fractions (Tack and Verloo, 1996).

Sample analysis using molecular-level analytical methods, such as synchrotron based X-ray absorption microspectroscopy, can provide more accurate determinations of solid phase fractionation, co-occurrence of elements and contaminant metal(loid) binding mechanisms (Walker et al., 2009). X-ray microspectroscopy has been previously employed to identify differences in Zn speciation between untreated soil and soil amended with fly ash and compost 12 years after the treatment (Nachtegaal et al., 2005). Using extended X-ray adsorption fine structure (EXAFS) spectroscopy, authors identified formation of poorly crystalline Zn-mineral phases in studied soils that would otherwise be very difficult to distinguish. Due to the heterogeneity of mine spoils and the fact that a small amount of material is analyzed using X-ray microspectroscopy, these results have a qualitative nature. Direct analyses using X-ray absorption microspectroscopy (qualitative data), however, can be used to interpret sequential selective dissolution results (quantitative data) when studying complex matrices of environmental samples.

Several studies have been implemented in order to identify the best combination of spoil amendments to reduce ecological risks related to As and metal mobility, spoil acidity and nutrient deficiency in order to establish vegetative cover on spoils generated at the Jales gold mine in Portugal (Bleeker et al., 2002, 2003; Mench et al., 2003). A combination of compost, zerovalent iron grit and coal fly ash (CZA) was identified to be the most effective at increasing microbial biomass and activity, key soil enzyme activities, and plant species richness six years after treatment (Renella et al., 2008). However, the amendments did not reduce As leaching. The aim of this study was to evaluate the potential risks for As mobilization in the vegetated mine spoil based on identification of changes in As speciation and fractionation as affected by ten years of aided phytostabilisation. Selective dissolution procedures and synchrotron-based X-ray microspectroscopy were applied to CZA treated and vegetated spoils in parallel to the untreated spoils.

## 2. Materials and methods

### 2.1. Spoil and amendments

Collection of mining spoils from the no longer operable (closed in 1992) Jales gold mine, Portugal, preparation and storage conditions of outdoor lysimeters

(0.125 m<sup>3</sup> vats equipped with a 20 cm compensation zone resulting in a 0.8 m<sup>2</sup> surface) that were exposed to natural climatic conditions (average annual temperature 12.5 °C, min 3–15 °C, max 9–27 °C, precipitation 870 mm y<sup>-1</sup>, sunlight 5.7 h) at the Villenave d'Ornon, Bordeaux, France, are described in detail in Mench et al. (2003). Schematic representation of the lysimeter set-up is given in Fig. 1. The spoils are residues of silver and gold ore composed mainly of quartz and various sulphides containing Fe, As, Pb, Cu and Zn (Santos Oliveira and Freira Avila, 1995).

The spoil was amended in 1998 with 5 dwt% (dry weight percent) compost + 5 dwt% coal fly ash + 1 wt% Fe<sup>0</sup> (zerovalent iron grit) by mixing in a cement blender and filling the 1 m<sup>3</sup> lysimeters.

Initial concentrations of elements in spoil at the start of the experiment prior to treatment in 1998 were: (in mg kg<sup>-1</sup>) As 1325; Cd 3.8; Cu 40; Ni 14; Pb 70; Zn 216. The starting composition of cyclonic or, more generally, fly ash from coal refuse burning in Beringen (also called beringite) was as follows: (in %) SiO<sub>2</sub> 51; Al<sub>2</sub>O<sub>3</sub> 31; CaO 4.14; K<sub>2</sub>O 2.56; MgO 1.44; Fe<sub>2</sub>O<sub>3</sub> 4.27; (in mg kg<sup>-1</sup>) S 4795; Mn 853; Zn 153; Cu 64; Pb 35; Ni 35; Cr 32; As 21; Co 13; Cd 2.3 and pH = 9.3 (Ruttens et al., 2006). The starting composition of the compost made from domestic and garden organic wastes and obtained from Intercompost, Bilzen, Belgium, was: (in mg kg<sup>-1</sup>) As 12.7; Cd 0.9; Cu 40.2; Ni 14.1; Pb 70.4; Zn 216. Iron grit was initially composed of 97% Fe<sup>0</sup>; 0.8% Mn and minor amounts of other impurities (Ni, Zn). Contribution of amendments to the total As content in the treated spoil was negligible (~1–2 mg kg<sup>-1</sup>).

Three sub-samples of ca 1 kg each of treated and untreated spoils were collected from lysimeters ten years later (2008) with a small stainless drill from the 0–20 cm soil depth layer, mixed, and stored in plastic containers (4 °C). Elemental composition of the spoils was measured with ICP-OES (Optima 2000DV, PerkinElmer) after digesting 2 g of air-dried sample in 15 mL aqua regia using a microwave digester (CEM Microwave Sample Preparation System, MARS 5). The required sample size was acquired by dividing air-dried samples with a riffle splitter. A *t*-test was used to compare mean element concentrations (*n* = 3) at 95% confidence level.

Arsenic speciation (As(III), As(V) and organic As species) in spoils was performed by an accredited laboratory (ALS Scandinavia AB, Sweden) using HPLC–HG–ICP–MS system after extracting 1 g of the material in 10 mL of 7 mM phosphate buffer (pH 8) in an ultrasonic bath for 30 min (Georgiadis et al., 2006).

### 2.2. Collection and analysis of biomass

Pine needles and litterfall from lysimeters with untreated and CZA treated spoils were collected and analyzed for elemental content. Litterfall over the topsoil was collected on the 0.5 m × 0.5 m surface of the leaching system placed in the middle of the lysimeters with untreated and CZA treated spoils. Individual senescent pine needles were separated by hand from the organic mat colonized by the fungi of the treated spoil. Air-dried samples were ground in a Tecator grinder and analyzed in duplicates. Weighed aliquots (0.5 g DW) were wet digested using a CEM MarsXpress microwave digestion system, with 5 mL 14 M HNO<sub>3</sub> and 2 mL 30% H<sub>2</sub>O<sub>2</sub> (180 °C, 20 min). Certified reference material (BIPEA maize V463) and blank reagents were included in the series. Elemental concentrations in digests were determined by ICP-AES (Varian Liberty 200).

### 2.3. Synchrotron X-ray microbeam analyzes

All  $\mu$ XRF and  $\mu$ XANES spectroscopy measurements were performed using the microprobe beamline X27A at the National Synchrotron Light Source (NSLS), Upton, NY. Aliquots from the preserved spoil samples described above were dispersed in a thin, single grain layer on a high purity silica disc and sealed with a polypropylene film. Samples were secured to an *x, y, z* motorized stage 45° to the incident beam and 13-element HGe Canberra fluorescence detector. The beam spot-size on the sample was maintained at ca. 15 × 10  $\mu$ m. Initially, two-dimensional XRF maps (incident energy 13 keV, 0.01 mm *x, y* step size) recorded As and Fe fluorescence. Element distributions (background subtracted, integrated peak intensity) were used to identify regions of interest to collect  $\mu$ XANES point spectra. A Si(111)

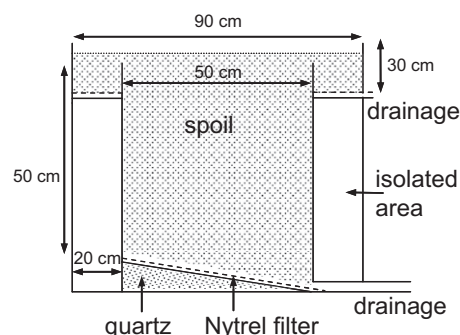


Fig. 1. Schematic presentation of the lysimeter lay-out.

monochromator crystal was used during all  $\mu$ XRF mapping and As  $\mu$ XANES spectra collection (0.15 eV step size through the edge region), and a Si(311) monochromator was used during all Fe  $\mu$ XANES spectra collection (0.1 eV step size through the edge region). Scorodite ( $\text{FeAsO}_4 \cdot 2\text{H}_2\text{O}$ ) and arsenolite ( $\text{As}_2\text{O}_3$ ) were used as arsenic standards, while ferrihydrite, goethite, hematite and magnetite were used as iron standards. XANES spectra were calibrated to the first-derivative maximum of a scorodite standard (11,874 eV) and the pre-edge peak maximum of a magnetite standard (7113.3 eV) for As and Fe, respectively. The collected XANES data were processed using Athena software (Ravel, 2008) including data normalization based on the Cromer–Lieberman calculations, background subtraction using the AUTOBK algorithm, alignment and merge of scans.

#### 2.4. Selective dissolution of Fe oxides

Differentiation of Fe oxides into amorphous and crystalline phases was performed using a sequential extraction procedure developed for sulfidic mine waste (Dold, 2003). The method was modified to improve extraction efficiency by increasing the time used to extract the poorly crystalline Fe(III) fraction from 1 to 2 h, in order to allow complete dissolution of ferrihydrite, which according to Cornell and Schwertmann (2003) is achieved in 2–4 h. Synthetic goethite powder was used as a reference material in the following extraction step. Since not all goethite was dissolved during the crystalline Fe(III) (oxyhydr)oxide dissolution step, an additional step was added designed to dissolve Fe–Mn oxides (Tessier et al., 1979). The residual Fe-fraction was assessed by dissolving the residue of the preceding step in aqua regia. The entire applied sequential extraction procedure was as follows:

- (1) Exchangeable fraction: 1 M  $\text{NH}_4$ -acetate pH 4.5 at liquid to solid ratio (L/S) 25, shaking for 2 h at room temperature (RT), followed by centrifugation at 1200 g for 15 min and rinsing with 10 mL of deionized water (centrifuged and discarded).
- (2) Poorly crystalline Fe(III)-oxyhydroxide fraction: 0.2 M  $\text{NH}_4$ -oxalate pH 3.0, L/S 25, shaking for 2 h at RT in darkness, centrifugation at 1200 g for 15 min. The washing step was adopted from Wenzel et al. (2001), i.e., the same  $\text{NH}_4$ -oxalate solution was used at L/S 12.5 and, after centrifugation and filtration, was combined with the previously extracted portion (making in total L/S 37.5).
- (3) Crystalline Fe(III) (oxyhydr)oxide fraction: 0.2 M  $\text{NH}_4$ -oxalate pH 3.0, L/S 25, heated in water bath at 80 °C for 2 h, centrifugation at 1200 g for 15 min, washing as in step (2).
- (4) Fe–Mn oxide fraction: 0.04 M  $\text{NH}_2\text{OH}$ –HCl in 25% (v/v) HO-acetate pH 2, L/S 20, heated in water bath at 96 °C for 6 h, centrifugation at 13 000 g for 30 min, washing with 10 mL deionized water (centrifuged and discarded). Fraction 3 and 4 were merged together into one fraction called crystalline Fe(III) (oxyhydr)oxides.
- (5) Organic matter and secondary sulphide fraction: 35%  $\text{H}_2\text{O}_2$ , heated in water bath at 85 °C for 1 h, L/S 25, centrifugation at 1200 g for 15 min, rinsing with 10 mL of deionized water (centrifuged and discarded).
- (6) Residual fraction: aqua regia ( $\text{HNO}_3$ :HCl, 1:3 v/v), L/S 15, in a microwave digester (CEM Microwave Sample Preparation System, Model MARS 5) at 195 °C for 10 min.

All extracts were filtered through 0.45  $\mu\text{m}$  cellulose acetate syringe filters and stored at 4 °C prior to analyses by ICP-OES.

### 3. Results and discussion

#### 3.1. Arsenic fractionation

Selective dissolution of spoil samples shows that the exchangeable As fraction and the poorly crystalline Fe(III)-oxyhydroxide bound As fraction are significantly smaller in the Compost, Zerovalent iron, and coal fly Ash (CZA) treated spoil relative to the untreated spoil (Fig. 2) indicating that As over time was depleted from these two fractions. The amount of As in the exchangeable fraction was reduced by nearly one half from 1128 to 635  $\text{mg kg}^{-1}$  in the CZA amended spoil. This depletion of exchangeable As fraction can be due to As shift to less soluble fractions or through exchanging sorbed As with competing ions present in fly ash and compost (e.g. phosphates, silicates) and consequent leaching. Both processes have occurred, i.e. a fraction of As became less soluble (increase in residual As fraction, Fig. 2) at the same time as increase in As leaching in treated spoil was observed (Renella et al., 2008). The decrease in total As content by 23% in CZA amended spoil compared to the untreated spoil supports the

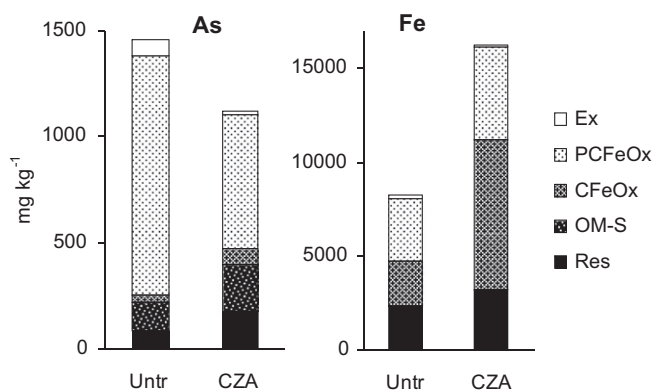


Fig. 2. Fractional distribution of As and Fe in untreated spoil and spoil treated with compost, zerovalent iron grit and coal fly ash (CZA). (Ex) Exchangeable fraction, (PCFeOx) Poorly crystalline Fe(III)-oxyhydroxides, (CFeOx) crystalline Fe(III)-(oxyhydr)oxides, (OM-S) organic matter and secondary sulphides, (Res) residual fraction.

assumption that a considerable amount of As was lost e.g. through leaching (Table 1).

Arsenic in ferrihydrite-bound fraction is less sensitive to the competing inorganic ions, but can be dissolved by organic acids, e.g. added with the compost. Organic matter is reported among the factors increasing As mobility in soil and mine tailings (Mench et al., 2003; Tye et al., 2002; Lee et al., 2009), although several authors argue that the evidence cited in support of OM-induced desorption or displacement of significant quantities of As in soils is inconclusive (Wenzel et al., 2001; Fitz and Wenzel, 2002). Nevertheless, organic molecules (e.g. oxalic, malic, phenolic acids) exuded by plant roots and established ion gradients in the rhizosphere has been demonstrated to promote the desorption of mineral-bound As (Gonzaga et al., 2009; Quartacci et al., 2009). Competition between OM and As for sorption sites as well as formation of ternary complexes of As-cationic metal-OM in

Table 1

Selected initial characteristics of spoil and elemental composition of untreated spoil and spoil treated with compost, zerovalent iron and fly ash (CZA) 10 years after the start of the remediation experiment.

	Untreated spoil	Spoil with CZA
Sand (%)	83.6	n.a.
Silt (%)	12.8	n.a.
Clay (%)	0.36	n.a.
Organic carbon (%)	0.045	n.a.
CEC ( $\text{cmol kg}^{-1}$ )	0.9	n.a.
pH	4.2	7.3
<i>Elements (mg kg<sup>-1</sup> DW, n = 3, <math>\pm</math>SD)<sup>a</sup></i>		
Al	6241 $\pm$ 575	13 106 $\pm$ 2256
As	1457 $\pm$ 89 <sup>b</sup>	1120 $\pm$ 40 <sup>b</sup>
Ca	1531 $\pm$ 48	1691 $\pm$ 64
Cr	2.9 $\pm$ 0.1	23.3 $\pm$ 0.5
Cu	12.4 $\pm$ 0.8	29.1 $\pm$ 6.0
Fe	8258 $\pm$ 493 <sup>b</sup>	16 242 $\pm$ 1006 <sup>b</sup>
K	2193 $\pm$ 232	2925 $\pm$ 507
Mg	1078 $\pm$ 57	1341 $\pm$ 73
Mn	151.5 $\pm$ 10.6	275.6 $\pm$ 8.5
Na	121.9 $\pm$ 11.3	189.2 $\pm$ 28.3
Ni	0.8 $\pm$ 0.1	10.0 $\pm$ 0.3
Pb	163.0 $\pm$ 5.4	128.7 $\pm$ 5.6
Zn	47.7 $\pm$ 3.5	156.3 $\pm$ 9.6
S	761.7 $\pm$ 80.7 <sup>b</sup>	1106.5 $\pm$ 132.9 <sup>b</sup>
P	672.4 $\pm$ 29.5	666.8 $\pm$ 46.9

<sup>a</sup> Except for K and P, all differences between element concentrations in untreated and CZA-treated spoils were statistically significant at 95% confidence level. n.a. – not analyzed.

<sup>b</sup> Calculated from sequential extraction results.

solution were suggested to be the principle mechanisms describing the association of between OM and As (Redman et al., 2002).

Although As associated with crystalline Fe phases increased in the treated spoil from  $38 \pm 4$  to  $76 \pm 17$  mg kg<sup>-1</sup>, it was the second smallest fraction after the exchangeable one in both spoils. Concentration of As increased twofold in the organic or residual sulfide fraction of the CZA spoil most likely due to its association with newly generated organic matter and microbial biomass. The CZA amended spoil contained 5 wt% compost and significantly higher microorganism population than the untreated spoil (Renella et al., 2008).

The amount of As in the residual fraction, which represents sparingly soluble As-containing mineral phases, also doubled in the treated spoil ( $180 \pm 13$  mg kg<sup>-1</sup>) relative to the untreated spoil ( $87 \pm 31$  mg kg<sup>-1</sup>). The presence of As-containing minerals can be seen from XANES results. The 'CZA 6' spectrum collected in treated spoil (Fig. 3a, 'CZA 6') has some features in the region of 11 880 to 11 900 eV, which are characteristic of crystalline As-containing mineral phases (e.g. scorodite Fig. 3a; Cancès et al., 2005; 2008). The occurrence of both pre-edge and post-edge features is consistent with the presence of residual sulphidic As minerals (arsenopyrite) mixed with oxidised minerals (e.g. scorodite) (Foster et al., 1998). A build-up of new As–S phases can be excluded seeing as sulfur concentration in the residual fraction remained unaltered by the spoil treatment ( $63 \pm 6$  vs  $65 \pm 18$  mg kg<sup>-1</sup>). The residual fraction of CZA spoil contained higher As:Fe molar ratio than that in the untreated spoil suggesting the possibility of the presence of new precipitate phases incorporating As and Fe in the residual fraction. Indeed, the As density on particle surface and molar As:Fe ratios in co-precipitates are higher than in surface-bound species and the precipitated As–Fe phases are more stable than surface-bound As (Fuller et al., 1993).

**Table 2**

Fresh biomass, mineral mass and concentration of As in litterfall samples.  $\pm$  SD,  $n = 2$ .

	Untreated spoil	CZA-treated spoil	
Mass of fresh litterfall (g m <sup>-2</sup> )	157.8	1722.4	
Mineral mass (mg m <sup>-2</sup> )	6.2 $\pm$ 0.3	312.0 $\pm$ 2.0	
	Pine needles + <i>H. lanatus</i> shoots	Pine needles	Mat colonized by hyphae
As concentration (mg kg <sup>-1</sup> DW)	40.5 $\pm$ 1.9	33.9 $\pm$ 5.8	422.4 $\pm$ 299.0
Non-digested residue (%)	4.3 $\pm$ 0.1	2.0 $\pm$ 1.0	8.7 $\pm$ 1.8 <sup>a</sup>

<sup>a</sup> The highest percentage of residues found in the mat sample (9.96%) corresponds to 132 mg kg<sup>-1</sup> residual As.

### 3.2. Impact of vegetation on arsenic fractionation

A substantial As concentration was detected in the CZA litterfall mat colonized by yellow fungal hyphae ( $210\text{--}530$  As mg kg<sup>-1</sup> DW), which was on average 12 times higher than in the needle fraction of the dominant plant *P. pinaster* growing in the CZA treated lysimeter (Table 2). The fungus was identified as *Rhizopogon roseolus* (Corda) Th. Fr., which is a frequent mycorrhizal association of maritime pine (*P. pinaster*).

The estimated As mineral mass in the litterfall was about 50-fold higher in the CZA treated spoil compared to the untreated spoil where only a few individual *H. lanatus* plants have survived. The establishment of As tolerant plant species in the CZA treated spoil (*Pinus pinaster*, *Holcus lanatus*, *Cotoneaster* sp. *Hedera helix*, *Deschampsia* sp., *Taraxacum officinalis*, *Erigeron canadensis*, *Celtis* sp.) appears to have significantly contributed to the As depletion by extracting As from the Fe-oxyhydroxide bound fraction. The dominant plant in the treated spoil alone, *P. pinaster*, has been shown to exude up to 400 mg g<sup>-1</sup> DW oxalic acid and smaller

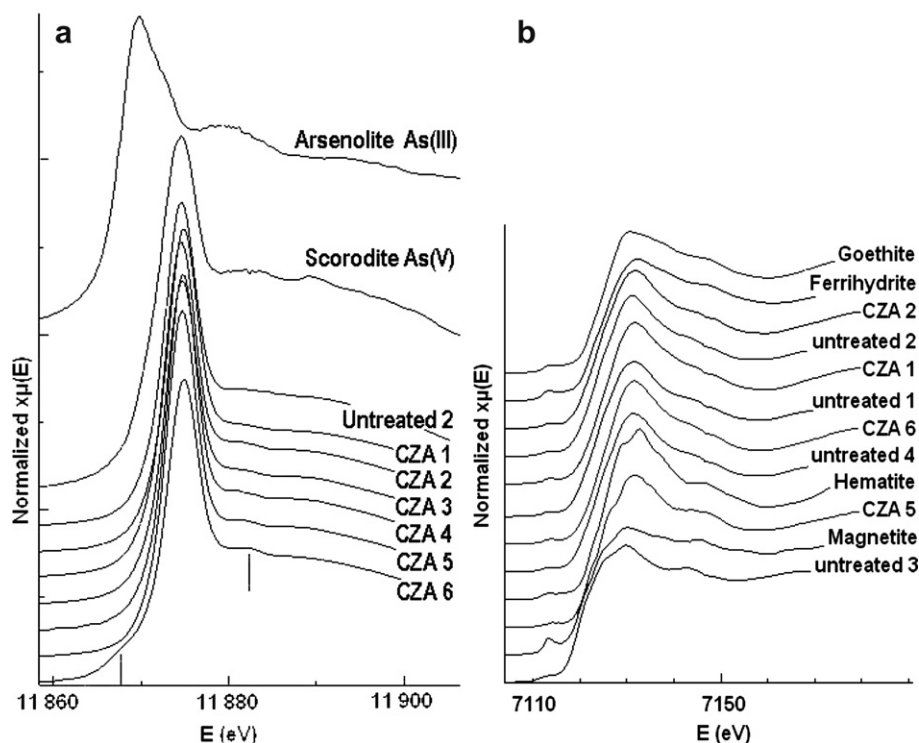


**Fig. 3.** Normalized (a) As and (b) Fe K-edge  $\mu$ XANES spectra of untreated spoils and spoils treated with compost, zerovalent iron grit and coal fly ash (CZA) and XANES spectra of reference compounds. Numbers indicate scans collected at representative locations of the treated sample (Fig. 4) and the untreated sample (Fig. 5).

amounts of malic, malonic and tartaric acids (Quartacci et al., 2009). These organic compounds, especially oxalic acid, can solubilize poorly crystalline ferrihydrite and facilitate the uptake of associated elements, i.e. those present in other than exchangeable fractions. Gonzaga et al. (2006) made similar observations in their study of As uptake by two plant species: most of the As was taken up from the ferrihydrite bound-As fraction, which was also the most abundant As fraction in their soil, rather than from the most available (exchangeable) fraction.

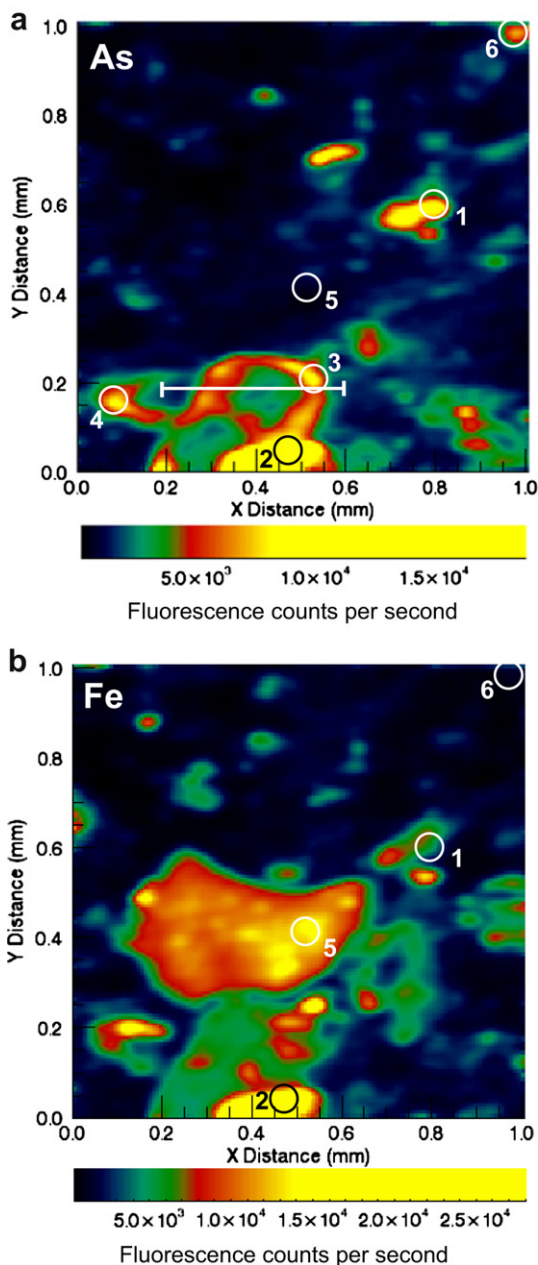


**Fig. 4.**  $\mu$ XRF images of (a) As and (b) Fe of the same grains within samples of the treated spoil. Color scale bars are shown with fluorescence counts per second to approximate relative concentrations of As and Fe. Numbers within each image indicate regions where XANES scans were collected (Fig. 3). (For interpretation of the references to colour in this figure legend, the reader is referred to the web version of this article.)

### 3.3. Arsenic speciation and association with Fe-(hydr)oxides

Two dimensional microprobe X-ray fluorescence ( $\mu$ XRF) images show that As fluorescence varies widely within the spoil samples, although low levels of As are distributed throughout both CZA treated spoils (Fig. 4a) and untreated spoils (Fig. 5a). Arsenic XANES spectra collected at a series of representative points within the  $\mu$ XRF images indicate that As(V) species dominate regardless of the As concentration (Fig. 3a). A minority of spots produced spectra with a shoulder located at 11 867 eV and a corresponding decrease in peak height of the As(V) adsorption edge (Fig. 3a, 'CZA 6', Fig. 6). Linear combination fitting using the two model compound spectra for As(III) and As(V) (Fig. 3a) indicates an As(V):As(III) ratio of 90:10% in this spot, which represented the highest relative As(III) concentration observed in both the treated and untreated spoils. Arsenic speciation in spoil extractions also indicate the dominance of As(V) species in treated and untreated samples. With this method, no other As species were detected and concentrations of As(III), monomethylarsonate (MMA) and dimethylarsinate (DMA) were below detection limits ( $<0.5$ ;  $<0.1$  and  $<0.2$  mg kg<sup>-1</sup>, respectively). Hence, the increased amount of organic matter, microbial population and vegetation in CZA spoil had no impact on the As oxidation state.

Most of the regions in the  $\mu$ XRF images with the highest As fluorescence ('As hotspots') were correlated with high Fe fluorescence counts (Fig. 4). Majority of the collected As XANES spectra had post-edge regions without significant features from 11 880 to

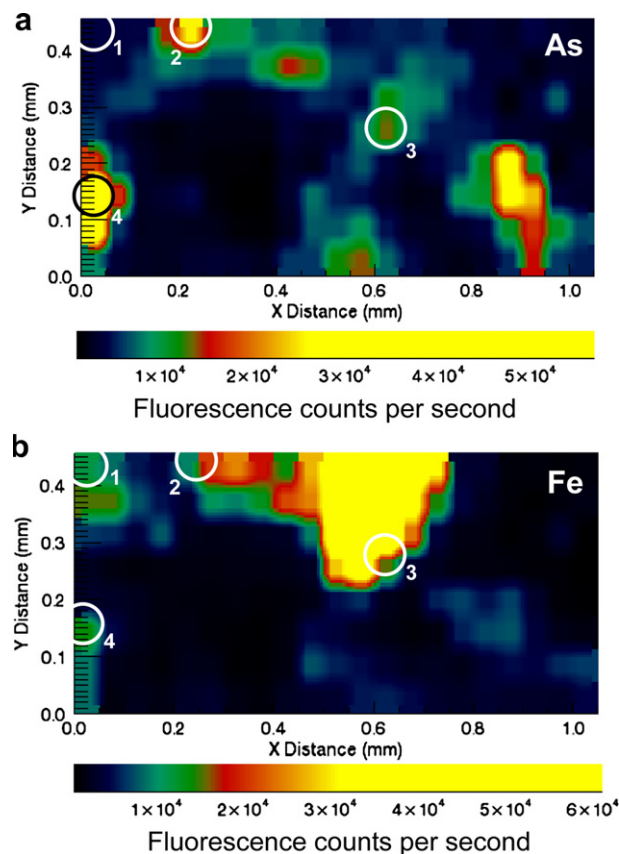


**Fig. 5.**  $\mu$ XRF images of (a) As and (b) Fe in untreated spoil sample. Color scale bars are shown with fluorescence counts per second to approximate relative concentrations of As and Fe. Numbers within each image indicate regions where XANES scans were collected (Fig. 3). (For interpretation of the references to colour in this figure legend, the reader is referred to the web version of this article.)

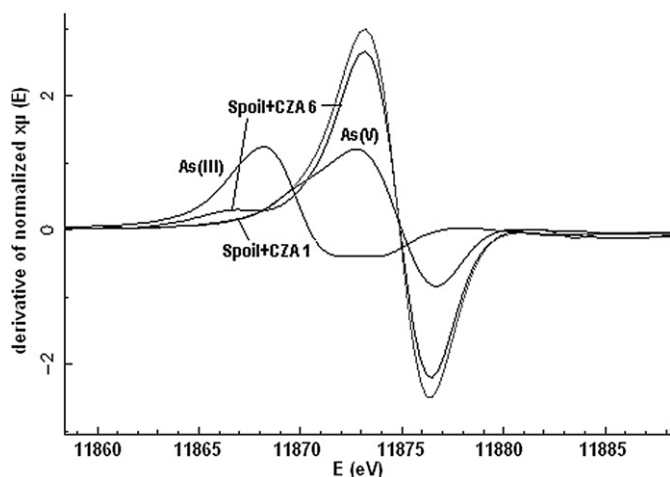


**Fig. 6.** Derivative of normalised As K-edge bulk XANES spectra of spoils treated with compost, zerovalent iron grit and coal fly ash (CZA) collected at regions 6 and 1 (Fig. 3) in comparison to the spectra of reference monocompounds As(III) and As(V).

11 900 eV suggesting the absence of crystalline As-containing minerals in those spots (Cancès et al., 2008). A line scan of As fluorescence taken across a representative As-containing particle shows that peaks in As fluorescence ring the edge of the particle (Fig. 7). The As:Fe fluorescence ratio is also significantly greater within the particle surface region, suggesting that As is concentrated at the particle surface as the As–Fe surface precipitate phase. The differentiation between surface adsorbed phases and amorphous surface precipitates either by the dissolution methods or mineralogical characterization are particularly difficult in bulk samples, but was possible with high-resolution  $\mu$ XRF imaging.

The CZA spoil treatment resulted in a doubling of the total Fe content in the spoil from 0.8 to 1.6 g kg<sup>-1</sup>, as analyzed 10 years after treatment. Selective dissolution of Fe oxides (Fig. 2) indicate that poorly crystalline Fe-oxyhydroxides (ferrihydrite) dominate in the untreated spoil (41%), while crystalline Fe(III) (oxyhydro)oxides (e.g. goethite, lepidocrocite, hematite) are the main Fe minerals in the treated spoil (49.3%). The amount of crystalline Fe(III)-phases in the treated spoil exceeded that of the untreated spoil more than three-fold (8008 vs 2304 mg kg<sup>-1</sup>), while the difference in poorly crystalline Fe(III)-oxyhydroxides was only 45% (4887 vs 3366 mg kg<sup>-1</sup>).

Iron K-edge XANES spectra collected at a series of representative points throughout the  $\mu$ XRF images (cf. numbers in Figs. 4 and 5b)

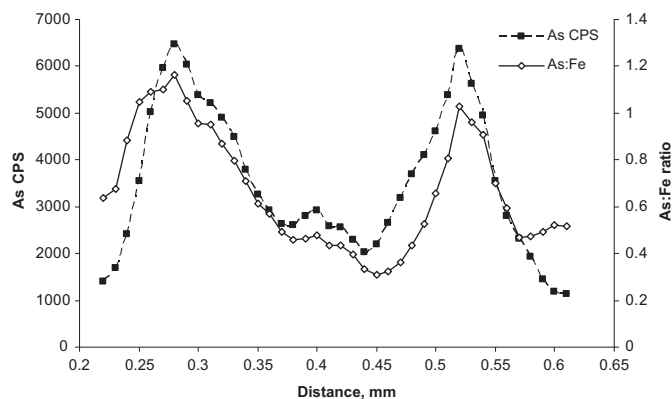


**Fig. 7.** A line scan of As fluorescence intensity (CPS – counts per second) taken across a representative As-containing particle (Fig. 3a) and the As:Fe fluorescence ratio.

show the ferrihydrite distribution throughout the samples (Fig. 3b). Fe oxide phases observed in both spoils, represented by spectra ‘CZA 5’ and ‘untreated 3’ (Fig. 3b) had clearly different features than the remaining spectra. The spectrum ‘CZA 5’ collected in the middle of the large Fe-containing particle has the closest resemblance to the hematite spectra, (Fig. 4b, point 5), while the spectrum ‘untreated 3’ correspond to that of magnetite (Fig. 5b), suggesting that these Fe particles are more crystalline than the others. These Fe-containing particles are also unique among the particles shown in the  $\mu$ XRF images due to the relatively low amounts of associated As (Figs. 4 and 5a). These direct observations confirm the selective dissolution results of the relatively low As binding capacity of crystalline Fe-oxide phases in spoils. According to the selective dissolution, only a minor As fraction (2.6% in untreated spoil and 6.8% in treated spoil) is associated with crystalline Fe (oxyhydro)oxides (Fig. 2) and the dominant As fraction is that bound to poorly crystalline Fe-oxyhydroxides in both spoils. It confirms that higher Fe crystallinity gives lower As sorption efficiency.

Ferrihydrite formation is favored by a fast oxidation of metallic Fe in soil and is more likely to form than the more crystalline goethite and lepidocrocite phases when high concentrations of organic matter, silicates or other crystallization inhibitors are present (Schwertmann and Cornell, 2000; Churchman, 2000). The aging and transformation of ferrihydrite to more crystalline mineral phases has been shown to reduce sorption sites and result in As desorption (Fuller et al., 1993). The high As concentration in the spoils, however, is expected to passivate Fe-(hydr)oxide surfaces and thereby inhibit aging and crystallization processes (Paige et al., 1997). A previous X-ray absorption fine structure spectroscopy study of Fe–As precipitates formed in hydrometallurgical solutions did not observe transformation of ferrihydrite to crystalline goethite or hematite phases even after ten years of aging in oxic spoils (Moldovan et al., 2003). The substantial amount of crystalline Fe phases detected in the CZA treated spoil (Fig. 2, fraction CFeOx) indicate that aging processes are active despite all the inhibitors present. It is possible that the Fe crystallization have contributed to the earlier observed increase in As leaching from the treated spoil (Renella et al., 2008; Mench et al., 2003).

Although only a small amount of the material was used in  $\mu$ XRF mapping (1 mm<sup>2</sup>) and spectroscopy, the results were consistent with those of the sequential extraction showing the preferential association of As with amorphous Fe-(hydr)oxides as opposed to crystalline Fe-oxide phases. The techniques are complementary and, when combined, may increase the certainty of the results analyzing complex environmental matrixes.

### 3.4. Amendments and As stability

It is expected that spoil amendments would keep As immobile by decreasing the As concentration in labile fractions while increasing in more stable fractions. Indeed, As was depleted from the most available fractions in the treated spoil, but mainly through leaching and plant uptake, although the most stable (residual) As fraction in the treated spoil also increased compared to the untreated spoil. The spoil treatment significantly increased the amount of poorly crystalline Fe-oxyhydroxides and, hence, the quantity of sorption sites. However, the abundant Fe amendment, which has been shown to effectively immobilize As when added as the only amendment (Kumpiene et al., 2006), failed to prevent As mobilization and leaching. Furthermore, As binding with poorly crystalline Fe-oxyhydroxides does not inhibit As uptake by plants. Organic acids exuded by plant roots, e.g. oxalic acid, can solubilize poorly crystalline ferrihydrite. Facilitating plant establishment on As contaminated spoils treated with Fe might therefore enhance As circulation in the spoil–plant–litter–spoil cycle. Further

development of the aided phytostabilization technique for As immobilization particularly selecting As excluders is necessary prior to its application on large scale field plots. Benefits of the method when a combination of soil amendments is used to facilitate vegetation establishment should therefore be carefully weighed over the possible negative impact to the environment, e.g. contamination of biomass and groundwater.

## Acknowledgments

This work was financially supported by The Swedish Research Council FORMAS. We gratefully acknowledge the National Synchrotron Light Source, Brookhaven National Laboratory (Upton, USA) for the use of beamlines X11A and X27A and Ing J. Guinbertau at MYCSA, INRA, Villenave d'Ornon for the assistance with the examination of fungi. J. Fitts and the NSLS are supported by US Department of Energy, Office of Science under contract DE-AC02-98CH10886.

## References

- Bleeker, P.M., Assunção, A.G.L., Teiga, P.M., de Koe, T., Verkleij, J.A.C., 2002. Revegetation of the acidic, As contaminated Jales mine spoil tips using a combination of spoil amendments and tolerant grasses. *Sci. Total Environ.* 300, 1–13.
- Bleeker, P.M., Teiga, P.M., Santos, M.H., de Koe, T., Verkleij, J.A.C., 2003. Ameliorating effects of industrial sugar residue on the Jales gold mine spoil (NE Portugal) using *Holcus lanatus* and *Phaseolus vulgaris* as indicators. *Environ. Pollut.* 125, 237–244.
- Cancès, B., Juillot, F., Morin, G., Laperche, V., Alvarez, L., Proux, O., Hazemann, J.L., Brown, G.E., Calas, G., 2005. XAS evidence of As(V) association with iron oxyhydroxides in a contaminated soil at a former arsenical pesticide processing plant. *Environ. Sci. Technol.* 39, 9398–9405.
- Cancès, B., Juillot, F., Morin, G., Laperche, V., Polya, D., Vaughan, D.J., Hazemann, J.L., Proux, O., Brown, G.E., Calas, G., 2008. Changes in arsenic speciation through a contaminated soil profile: a XAS based study. *Sci. Total Environ.* 397, 178–189.
- Carabante, I., Grahn, M., Holmgren, A., Kumpiene, J., Hedlund, J., 2009. Adsorption of As (V) on iron oxide nanoparticle films studied by in situ ATR–FTIR spectroscopy. *Colloid Surface A* 346, 106–113.
- Churchman, G.J., 2000. The alteration and formation of soil minerals by weathering. In: Sumner, M.E. (Ed.), *Handbook of Soil Science*. CRC Press, Boca Raton, pp. F3–F76.
- Cornell, R.M., Schwertmann, U., 2003. *The Iron Oxides: Structure, Properties, Reactions, Occurrences and Uses*. Wiley-VCH, Weinheim.
- Dold, B., 2003. Speciation of the most soluble phases in a sequential extraction procedure adapted for geochemical studies of copper sulfide mine waste. *J. Geochem. Explor.* 80, 55–68.
- Dzombak, D.A., Morel, F.M.M., 1990. *Surface Complexation Modeling: Hydrous Ferric Oxide*. Wiley, New York.
- Fitz, W.J., Wenzel, W.W., 2002. Arsenic transformations in the soil rhizosphere-plant system: fundamentals and potential application to phytoremediation. *J. Biotechnol.* 99, 259–278.
- Foster, A.L., Brown Jr., G.E., Tingle, T.N., Parks, G.A., 1998. Quantitative arsenic speciation in mine tailings using X-ray absorption spectroscopy. *Am. Mineral.* 83, 553–568.
- Fuller, C.C., Davis, J.A., Waychunas, G.A., 1993. Surface chemistry of ferrihydrite: part 2. Kinetics of arsenate adsorption and coprecipitation. *Geochim. Cosmochim. Acta* 57, 2271–2282.
- Georgiadis, M., Cai, Y., Solo-Gabriele, H.M., 2006. Extraction of arsenate and arsenite species from soils and sediments. *Environ. Pollut.* 141, 22–29.
- Gonzaga, M.I.S., Santos, J.A.G., Ma, L.Q., 2006. Arsenic chemistry in the rhizosphere of *Pteris vittata* L. and *Nephrolepis exaltata* L. *Environ. Pollut.* 143, 254–260.
- Gonzaga, M.I.S., Ma, L.Q., Santos, J.A.G., Matias, M.I.S., 2009. Rhizosphere characteristics of two arsenic hyperaccumulating *Pteris* ferns. *Sci. Total Environ.* 407, 4711–4716.
- Hartley, W., Edwards, R., Lepp, N.W., 2004. Arsenic and heavy metal mobility in iron oxide-amended contaminated soils as evaluated by short- and long-term leaching tests. *Environ. Pollut.* 131, 495–504.
- Hector, C.M., Rainer, S., 2010. The Cartagena – La union mining district (SE Spain): a review of environmental problems and emerging phytoremediation solutions after fifteen years research. *J. Environ. Monitor.* 12, 1225–1233.
- Jain, A., Ravan, K.P., Loeppert, R.H., 1999. Arsenite and arsenate adsorption on ferrihydrite: surface charge reduction and net OH-release stoichiometry. *Env. Sci. Technol.* 33, 1179–1184.
- Kumpiene, J., Ore, S., Renella, G., Mench, M., Lagerkvist, A., Maurice, C., 2006. Assessment of zerovalent iron for stabilization of chromium, copper, and arsenic in soil. *Environ. Pollut.* 144, 62–69.
- Lee, G.-U., Lee, S.-W., Chon, H.-T., Kim, K.-W., Lee, J.-S., 2009. Enhancement of arsenic mobility by indigenous bacteria from mine tailings as response to organic supply. *Environ. Int.* 35, 496–501.
- Lottermoser, B.G., 2003. *Mine Wastes: Characterization, Treatment and Environmental Impacts*. Springer-Verlag, Berlin.
- Mench, M., Bussièrre, S., Boisson, J., Castaing, E., Vangronsveld, J., Ruttens, A., De Koe, T., Bleeker, P., Assunção, A., Manceau, A., 2003. Progress in remediation and revegetation of the barren Jales gold mine spoil after in situ treatments. *Plant Soil* 249, 187–202.
- Meng, X., Bang, S., Korfiatis, G.P., 2000. Effects of silicate, sulfate, and carbonate on arsenic removal by ferric chloride. *Wat. Res.* 34, 1255–1261.
- Moldovan, B.J., Jiang, D.T., Hendry, M.J., 2003. Mineralogical characterization of arsenic in uranium mine tailings precipitated from iron-rich hydrometallurgical solutions. *Environ. Sci. Technol.* 37, 873–879.
- Nachtegaal, M., Marcus, M.A., Sonke, J.E., Vangronsveld, J., Livi, K.J.T., van der Lelie, D., Sparks, D.L., 2005. Effects of in situ remediation on the speciation and bioavailability of zinc in a smelter contaminated soil. *Geochim. Cosmochim. Acta* 69, 4649–4664.
- Paige, C.R., Snodgrass, W.J., Nicholson, R.V., Schärer, J.M., 1997. An arsenate effect on ferrihydrite dissolution kinetics under acidic oxic conditions. *Water Res.* 31, 2370–2382.
- Pedersen, H.D., Postma, D., Jakobsen, R., 2006. Release of arsenic associated with the reduction and transformation of iron oxides. *Geochim. Cosmochim. Acta* 70, 4116–4129.
- Quartacci, M.F., Irtelli, B., Gonnelli, C., Gabbriellini, R., Navari-Izzo, F., 2009. Naturally-assisted metal phytoextraction by *Brassica carinata*: role of root exudates. *Environ. Pollut.* 157, 2697–2703.
- Ravel, B., 2008. *ATHENA User's Guide*. Version 1.5.
- Redman, A.D., Macalady, D.L., Ahmann, D., 2002. Natural organic matter affects arsenic speciation and sorption onto hematite. *Environ. Sci. Technol.* 36, 2889–2896.
- Renella, G., Landi, L., Ascher, J., Ceccherini, M.T., Pietramellara, G., Mench, M., Nannipieri, P., 2008. Long-term effects of aided phytostabilisation of trace elements on microbial biomass and activity, enzyme activities, and composition of microbial community in the Jales contaminated mine spoils. *Environ. Pollut.* 152, 702–712.
- Ruttens, A., Mench, M., Colpaert, J.V., Boisson, J., Carleer, R., Vangronsveld, J., 2006. Phytostabilization of a metal contaminated sandy soil. I: influence of compost and/or inorganic metal immobilizing soil amendments on phytotoxicity and plant availability of metals. *Environ. Pollut.* 144, 524–532.
- Santos Oliveira, J.M., Freira Avila, E.P., 1995. Avaliação do Impacto Químico Ambiental Provocado por uma Exploração Mineira, Um caso de estudo na Mina de Jales. *Estud. Nota Trabalhos* 37, 25–50 pp.
- Schwertmann, U., Cornell, R.M., 2000. *Iron Oxides in the Laboratory: Preparation and Characterization*, second ed. Wiley-VCH, Weinheim.
- Sherman, D.M., Randall, S.R., 2003. Surface complexation of arsenic(V) to iron(III) hydroxides: structural mechanism from ab initio molecular geometries and EXAFS spectroscopy. *Geochim. Cosmochim. Acta* 67, 4223–4230.
- Tack, F.M.G., Verloo, M.G., 1996. Estimated solid phase distribution of metals released in the acid extractable and reducible steps of a sequential extraction. *Int. J. Environ. Anal. Chem.* 64, 171–177.
- Tessier, A., Campbell, P.G.C., Bisson, M., 1979. Sequential extraction procedure for the speciation of particulate trace metals. *Anal. Chem.* 51, 844–851.
- Tye, A.M., Young, S.D., Crout, N.M.J., Zhang, N., Preston, S., Bailey, E.H., Davison, W., McGrath, S.P., Paton, G.L., Kilham, K., 2002. Predicting arsenic solubility in contaminated soils using isotopic dilution techniques. *Env. Sci. Technol.* 36, 982–988.
- Vangronsveld, J., Van Assche, F., Clijsters, H., 1995. Reclamation of a bare industrial area contaminated by non-ferrous metals: in situ metal immobilisation and revegetation. *Environ. Pollut.* 87, 51–59.
- Vangronsveld, J., Ruttens, A., Mench, M., Boisson, J., Lepp, N.W., Edwards, R., Penny, C., van der Lelie, D., 2000. In situ inactivation and phytoremediation of metal/metalloid contaminated soils: field experiments. In: Wise, D.L., Trantolo, D.J., Cichon, E.J., Inyang, H.I., Stottmeister, U. (Eds.), *Bioremediation of Contaminated Soils*, second ed. Marcel Dekker, New York, pp. 859–884.
- Vangronsveld, J., Herzog, R., Weyens, N., Boulet, J., Adriaensens, K., Ruttens, A., Thewys, T., Vassilev, A., Meers, E., Nehnevajova, E., van der Lelie, D., Mench, M., 2009. Phytoremediation of contaminated soils and groundwater: lessons from the field. *Environ. Sci. Pollut. Res.* 16, 765–794.
- Walker, S.R., Parsons, M.B., Jamieson, H.E., Lanzirrotti, A., 2009. Arsenic mineralogy of near-surface tailings and soils: influences on arsenic mobility and bioaccessibility in the Nova Scotia gold mining districts. *Can. Mineral.* 47, 533–556.
- Wenzel, W.W., Kirchbaumer, N., Prohaska, T., Stingeder, G., Lombi, E., Adriano, D.C., 2001. Arsenic fractionation in soils using an improved sequential extraction procedure. *Anal. Chim. Acta* 436, 309–323.
- Winterhalder, K., 1996. Environmental degradation and rehabilitation of landscape around Sudbury, a major mining and smelting area. *Environ. Rev.* 4, 185–224.